Magnetic aftereffect spectroscopy of Fe- and Co-based amorphous alloys

P. Vojtanik* and R. Andrejco†
Institute of Physics, Fac. Sci., P.J. Šafárik University, Park Angelinum 9, 041 54 Košice, Slovakia
(Received 19 May 2006; revised manuscript received 27 October 2006; published 21 December 2006)

Theoretical and experimental fundamentals of a computer-based spectroscopic method–magnetic aftereffect (MAE) spectroscopy—giving sets of elementary activation energy (AE) spectra of magnetic relaxation (MR) processes, are introduced. Structural MRs in two representative amorphous alloys, $Fe_{75}Si_{15}B_{10}$ and $Co_{70}Fe_5Si_{15}B_{10}$, were investigated by MAE spectroscopy. The MAE measurements were performed on the as-cast and annealed samples in a temperature range of 77–620 K. Activation parameters of the individual directional reordering processes were obtained. The B- and Si-type MRs were identified in the FeSiB and CoFeSiB alloys. The B-type MRs originate from the reorientation of Co-B or Fe-B atom pairs. The Si-type MRs come from the reorientation of Co-Si or Fe-Si pairs. Atom pairs Fe-B, Co-B, Fe-Si, and Co-Si are aligned by the increasing values of the most probable activation energies (AE) of the MR. For the B and Si types of the MR, the two most probable activation energies, $Q^*=1.33$ and 1.55 eV, with the pre-exponential factors $\tau_0=2\times10^{-15}$ and 6×10^{-16} s, respectively, were obtained in the as-cast FeSiB alloy. For the as-cast $Co_{70}Fe_5Si_{15}B_{10}$ alloy, the B and Si types of the MR are characterized by the activation energies $Q^*=1.38$ and 2.16 eV and the pre-exponential factors $\tau_0=8\times10^{-16}$ and 9×10^{-18} s, respectively. Low temperature annealing causes lowering of the MAE peaks and shifts the peak temperatures and the AEs of MRs in both alloys to higher values. The MAE and AE spectra of the annealed CoFeSiB amorphous alloy exhibit one peak only.

DOI: 10.1103/PhysRevB.74.224427 PACS number(s): 75.60.Lr, 75.50.Kj, 81.40.Ef

INTRODUCTION

Comparative studies on magnetic properties and stability of amorphous alloys based on Fe (high induction) and Co (nearly zero magnetostriction) are interesting from technological and theoretical points of view.[1–5] Technically important requirements for magnetic materials are excellent magnetic properties and good magnetic stability, which is influenced by structural stability.

The diffusion magnetic aftereffect (MAE) observed in all amorphous soft magnetic alloys is a manifestation of the structural magnetic relaxation (MR). According to the micromagnetic theory,[6,7] the MAE is caused by the directional reordering of mobile atom pairs in the alloy governed by the local direction of magnetization. MAE spectroscopy affords theoretically and practically important thermodynamic characteristics of soft magnetic materials: activation energy (AE) spectra and pre-exponential factors. We have used MAE spectroscopy for investigation of the structural MR caused by the directional reordering of Fe-B, Fe-Si, Co-B, and Co-Si atom pairs in the amorphous $Fe_{75}Si_{15}B_{10}$ and $Co_{70}Fe_5Si_{15}B_{10}$ alloys which represent typical Fe- and Co-based amorphous alloys. The FeSiB alloy possesses high magnetostriction and high magnetization. The CoFeSiB alloy with nearly zero magnetostriction exhibits high permeability and low coercivity.

The micromagnetic model in Refs. 6 and 7 is frequently used for the analysis of the MAE spectra, but it assumes reorientations of arbitrary atom pairs in the alloy. We have extended it in an effort to distinguish between contributions of different atom pairs to the MAE and to find relationships between the MAE-spectrum shape and the alloy composition.[8] This approach is different in the transition from magnetic relaxation originating from the directional reordering of arbitrary atom pairs to the directional reordering of specific pairs with defined composition. The directional reordering of atom pairs can significantly influence the magnetic properties of alloys as well as their structural stability. The knowledge of these processes can be helpful for the analyses of all phenomena where directional ordering is of some importance.

The MAE phenomenon in amorphous alloys is attributed to reorientations of anisotropic point defects and their clusters minimizing their free energy. Reorientations of the atom pairs around the vacancies affect a time-temperature dependence of the initial reluctivity ($r=1/\chi$, χ susceptibility). In a simple model it is assumed that in the vicinity of the free volume an atom pair may occupy two different orientations of its axis [Fig. 1(a)] with regard to the local direction of magnetization. The more favorable orientation is given by the lower value of the interaction energy

$$\varepsilon = \varepsilon_0 \cos^2 \varphi, \tag{1}$$

where ε_0 is the interaction constant and φ is the angle between the atom pair axis and the local magnetization. The two orientations are separated by an energy barrier Q which may be overcome either by a thermal activation or by a tunnelling process. Such a transition can be illustrated by a double-well model [Fig. 1(b)].

As an example, assume a multicomponent alloy composed of transition ferromagnetic elements T_l and metalloids M_k, l, $k=1,2,\ldots$. Several types of nearest-neighbor atom pairs can be found in the vicinity of the free volume (e.g., T_1-T_2, T_1-M_1, T_1-M_2,...). Pairs M_k-M_l, k, $l=1,2,\ldots$ can be omitted because there is a very small probability that two metalloid atoms are occupying nearest-neighbor positions and because their interactions are not magnetic.

When an alloy consists of R different types of atom pairs, it is suitable to introduce R different two-level systems [Fig. 1(b)], each with characteristic distribution of activation parameters related to its own type of atom pairs.[8] Differences in two-level systems are also given by different magnetic

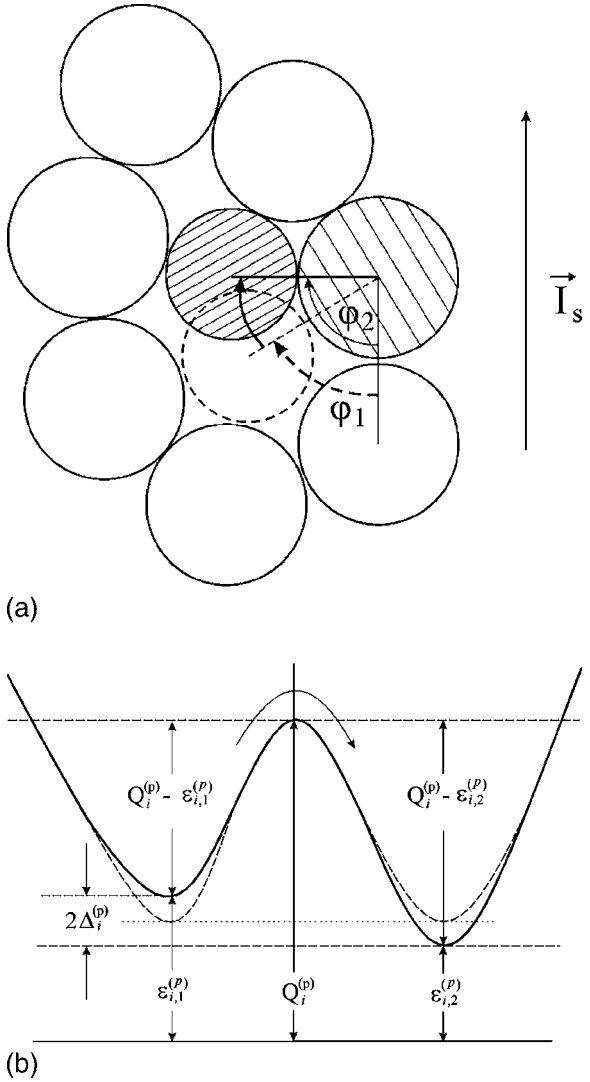

FIG. 1. (a) Minimization of the free energy of the system by reorientation of the atom pair axis during structural magnetic relaxation. $\vec{I}_S$ is the local magnetization, φ_1 is the initial angle, φ_2 is the final angle. (b) Two-level system for the local rearrangement of the ith p-type mobile atom pair by the thermal activation or a tunneling process. $2\Delta^{(p)}$ is the splitting energy, $Q^{(p)}$ is the activation energy for transition, $\varepsilon_{i,1}^{(p)}$ and $\varepsilon_{i,2}^{(p)}$ are the magnetic interaction energies in two pair axis orientations.

interaction energies between the pth atom pair type and the local magnetization

$$\varepsilon_{i,j}^{(p)} = \varepsilon_{i,j}^{(p)ex} + \varepsilon_{i,j}^{(p)K} + \varepsilon_{i,j}^{(p)el}, \quad i = 1 \ldots N_0^{(p)}, \quad j = 1,2, \quad (2)$$

where $p=1,\ldots,R$, $N_0^{(p)}$ is the number of mobile atom pairs of the pth type in the unit volume able to relax, and $\varepsilon_{i,j}^{(p)ex}$, $\varepsilon_{i,j}^{(p)K}$, $\varepsilon_{i,j}^{(p)el}$ are exchange, anisotropy, and magnetoelastic interaction energies of the ith p-type atom pair in the jth orientation, respectively. The first two interactions are disregarded in the magnetoelastic model of the MAE.[9,10] In the ferromagnetic state the magnetic interaction energy of an atom pair depends on its orientation (full curve), whereas in the paramagnetic state both orientations are equivalent (dashed curves). The splitting energy $2\Delta^{(p)}$ is composed of a structural term, $2\Delta_S^{(p)}$, and a magnetic term, $2\Delta_M^{(p)}$.

Below the Curie temperature the MR is driven by magnetic interactions. The splitting energy is changed predominantly via its magnetic term which is for ith atom pair of the pth type, defined as

$$2\Delta_{M,i}^{(p)} = \varepsilon_{i,1}^{(p)} - \varepsilon_{i,2}^{(p)}. \quad (3)$$

Redistributions of defects between two energy states of pair-axis orientations are described by a set of the rate equations

$$dN_j^{(p)}/dt = -\nu_{jj'}^{(p)} N_j^{(p)} + \nu_{jj'}^{(p)} N_{j'}^{(p)}, \quad p = 1,2,\ldots,P,$$

$$j \neq j', j, j' = 1,2. \quad (4)$$

Here $N_j^{(p)}$ and $N_{j'}^{(p)}$ are the numbers of occupied states in the unit volume in orientations 1 and 2, respectively. $\nu_{jj'}^{(p)}$ are jump frequencies for the pth atom pair type transition between the orientations j and j'. They can be expressed as

$$\nu_{jj'}^{(p)} = \nu_{00} e^{S_{jj'}^{(p)}/k} e^{-(Q^{(p)} - \varepsilon_{jj'}^{(p)})/kT}, \quad (5)$$

where ν_{00} denotes an attempt frequency of the order of the Debye frequency (10^{13} s^{-1}) and $S_{jj'}^{(p)}$ is the activation entropy for the transition $j \rightarrow j'$, k is Boltzmann's constant, and T is the absolute temperature. Assuming $\varepsilon_{jj'}^{(p)} \ll Q^{(p)}$ and $S_{jj'}^{(p)} = S_{j'j}^{(p)} = S^{(p)}$, which hold well in the case of two nearly equivalent configurations, then

$$\nu_{jj'}^{(p)} \equiv \nu^{(p)} = \nu_0^{(p)} e^{-Q^{(p)}/kT}. \quad (6)$$

The term $\nu_{00} \exp(S^{(p)}/k)$ was replaced by the pre-exponential factor $\nu_0^{(p)}$. Transitions between two levels in two-level systems are reversible. Instead of $\nu^{(p)}$, the Arrhenius formula for relaxation times

$$\tau^{(p)} = 1/\nu^{(p)} = \tau_0^{(p)} e^{Q^{(p)}/kT} \quad (6a)$$

is frequently used, where the pre-exponential factor $\tau_0^{(p)} = \nu_{00}^{-1} \exp(-S^{(p)}/k)$. The solution of Eq. (4) for the pth atom pair type is

$$N_j^{(p)}(\Delta^{(p)}, t) = \frac{N_0^{(p)}}{2}\left[1 - (-1)^j \mathrm{tgh}\frac{\Delta^{(p)}}{kT}(1 - e^{-t/\tau^{(p)}})\right], \quad j = 1,2. \quad (7)$$

It can be obtained assuming that two-level systems are uncoupled and at the time $t=0$ the initial condition $N_1^{(p)}(0)/2 = N_2^{(p)}(0)/2 = N_0^{(p)}/2$ holds. Equation (7) describes only reversible transitions in two-level systems. Reordering of the atom pairs influences the domain wall's stabilization potential whose steepness directly determines the domain wall's mobility. The stabilization potential of the domain wall is defined as

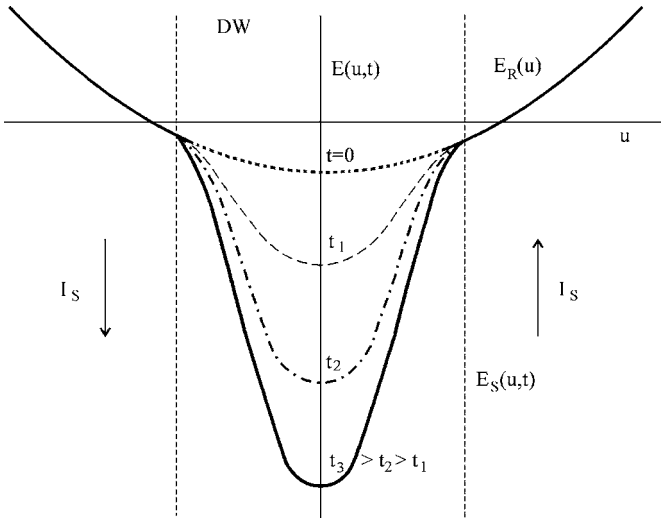

FIG. 2. Development of the domain wall's potential $E(u,t)=E_R(u)+E_S(u,t)$ during its stabilization caused by the magnetic relaxation (schematic design).

$$E_S(t)=\sum_{p=1}^{R}\sum_{i=1}^{N_0^{(p)}}\sum_{j=1,2}[N_j^{(p)}(z_i,t)-N_0^{(p)}]\varepsilon_{i,j}^{(p)}(z_i), \tag{8}$$

where $N_j^{(p)}(z_i,t)$ is the volume concentration of the mobile defects with the orientation j in the position z_i at time t after demagnetization. $\varepsilon_{i,j}^{(p)}$ is defined by Eq. (2).

Development of the stabilization potential, $E_S(u,t)$, and the total domain wall's potential, $E(u,t)$, respectively, are seen in Fig. 2. The curvature of the $E(u,t)$ bottom determines the initial reluctivity (susceptibility). The steepness of the $E(u,t)$ in the inflexion point determines the critical field H_{CR} of the perminvar effect[11] in the alloys after stabilization by the MR. "u" refers to a distance of the domain wall from its initial position. The reluctivity time change $\Delta r(t,T)$ can be finally expressed as

$$\begin{aligned}\Delta r(t)&=\frac{1}{\chi(t)}-\frac{1}{\chi_0}=\frac{1}{2FI_S^2}\frac{d^2E_S(u,t)}{du^2}\\&=\frac{2}{15F\delta_0 I_S^2}\sum_{p=1}^{R}\frac{\langle(\varepsilon_{eff}^{(p)})^2\rangle}{k\,.\,T}\left\langle\frac{1}{\cosh^2(\Delta_S^{(p)}/kT)}\right\rangle\\&\times N_0^{(p)}\int P^{(p)}(\tau^{(p)})(1-e^{t/\tau^{(p)}})d\tau^{(p)},\end{aligned} \tag{9}$$

where $\chi(t)$ and χ_0 are the initial susceptibilities at times t and $t=0$, respectively. F denotes the domain wall's area per unit volume, δ_0 is the domain wall's thickness, I_S is the saturation magnetization. The effective interaction constant $\langle(\varepsilon_{eff}^{(p)})^2\rangle$ is defined as

$$\langle(\varepsilon_{eff}^{(p)})^2\rangle=\langle(\varepsilon^{ex(p)})^2\rangle+\langle(\varepsilon^{K(p)})^2\rangle+\langle(\varepsilon^{el(p)})^2\rangle. \tag{2a}$$

$P^{(p)}$ is a distribution of the relaxation times $\tau^{(p)}$ of the p-type MR.

Equation (9) enables analysis of reversible reorderings of atom pairs of different chemical compositions. The MR process in an amorphous alloy is generally characterized by an asymmetric continuous spectrum of the AEs. A real continuous distribution function of the activation energies $P(Q)$ can be approximated by a stepwise set of the box-type distribution functions.[12] MAE spectroscopy is a suitable method for the experimental estimation of the AE spectra.

EXPERIMENTAL

The investigated amorphous alloys $Fe_{75}Si_{15}B_{10}$ and $Co_{70}Fe_5Si_{15}B_{10}$ were prepared by the rapid quenching method. The amorphicity was checked by x-ray diffraction. The Curie temperatures were obtained from the temperature dependences of the initial susceptibility; the crystallization temperatures were obtained by the resistance measurements (four-point method).

Both alloys were investigated in the as-cast and annealed states. The individual samples were annealed above their Curie temperatures (Table I) in an atmosphere of argon. The $Co_{70}Fe_5Si_{15}B_{10}$ alloy was annealed at 683 K for 30 min, the $Fe_{75}Si_{15}B_{10}$ alloy was annealed at 723 K for 30 min. The MAE spectra were measured by the MAE spectrometer [Fig. 3(a)] based on the LC oscillator technique[13] with the measuring field amplitude less than 0.1 A/m and frequencies around 10 kHz, according to the control program [Fig. 3(b)]. The MAE spectra consist of sets of the reluctivity isochrones

$$\frac{\Delta r}{r}=\frac{r(t_2,T)-r(t_1,T)}{r(t_1,T)}, \tag{10}$$

where $t_1=1$ s, $t_2=2$, 3, 5, 10, 20, 30, 60, 90, 120, and 180 s are the chosen times. The last isochrone ($t_2=180$ s) represents the whole MAE spectrum in the following text.

The MAE spectra were numerically analyzed by the Levenberg-Marquardt method with the model fitting function

TABLE I. Parameters of the MAE for as-cast (subscript AC) and annealed (AN) samples. Δr/r: magnetic relaxation intensity; τ_0: pre-exponential factor; Q^*: the most probable activation energy; T_{MAX}: the MAE-spectrum peak temperature; T_C: Curie temperature; and T_X: crystallization temperature.

Alloy	MR type	$(\Delta r/r)_{AC}$ (%)	$(\Delta r/r)_{AN}$ (%)	$\tau_{0,AC}$ (s)	$\tau_{0,AN}$ (s)	Q^*_{AC} (eV)	Q^*_{AN} (eV)	$T_{MAX,AC}$ (K)	$T_{MAX,AN}$ (K)	T_C (K)	T_X (K)
$Fe_{75}Si_{15}B_{10}$	B	27.0	9.7	2×10^{-15}	8×10^{-14}	1.33	1.46	411	513	713	780
	Si	41.8	14.7	6×10^{-16}	2×10^{-15}	1.55	1.81	467	562		
$Co_{70}Fe_5Si_{15}B_{10}$	B	16.8	11.3	8×10^{-16}	6×10^{-15}	1.38	1.50	430	500	681	743
	Si	4.9		9×10^{-18}		2.16		575			

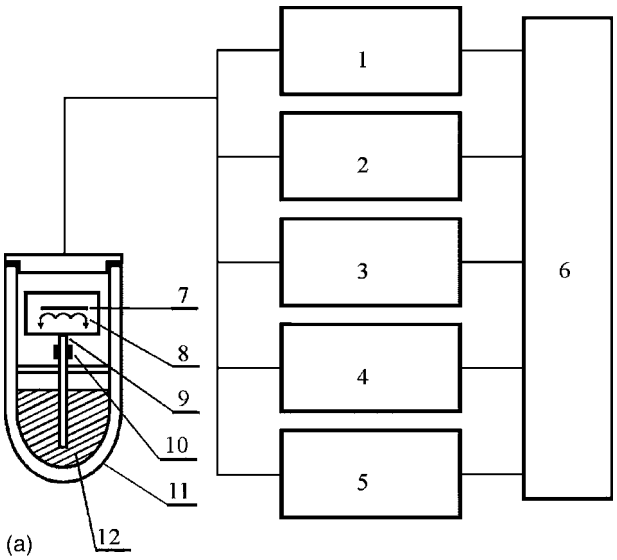

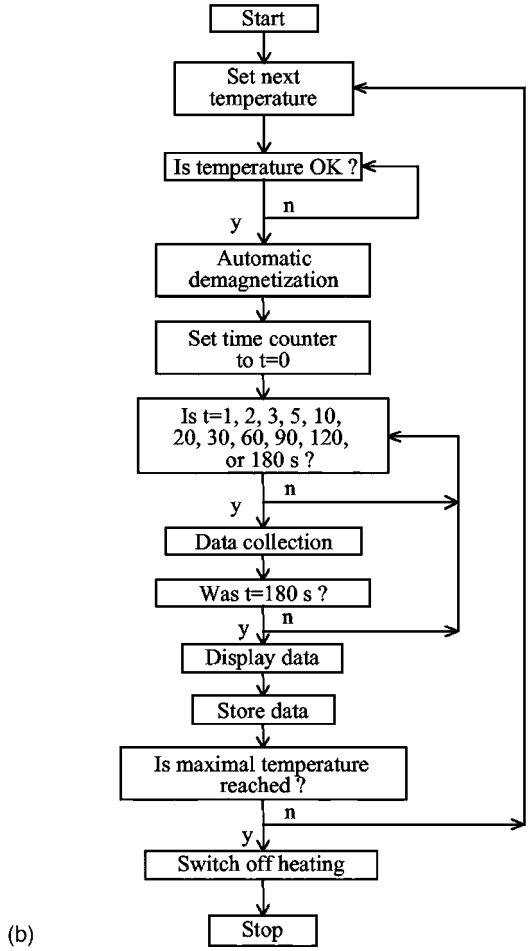

FIG. 3. (a) An apparatus for reluctivity MAE measurement. 1: demagnetizer; 2: reluctivity (susceptibility) meter; 3: temperature controller; 4: power supply; 5: voltmeter; 6: PC; 7: sample holder; 8: pick-up coil; 9: thermometer; 10: heater; 11: Dewar-vessel; and 12: LN_2. (b) A flow diagram of the MAE-spectra measurements.

$$\Delta r(t_1,t_2,T)=\sum_{p=1}^{R}\sum_{l=1}^{n}\Delta r_l^{(p)}\frac{\Delta Ei_l^{(p)}(t_2)-\Delta Ei_l^{(p)}(t_1)}{\ln(\tau_{l,2}^{(p)}/\tau_{l,1}^{(p)})}. \quad (11)$$

A computer analysis provides characteristic box-type AE spectra, $P(Q)$, with n steps and pre-exponential factors $\tau_0^{(p)}$. The number $R=2$ indicates that two particular MR processes are taken into account for the investigated alloys. The relaxation times are determined by the equations $\tau^{(p)}_{l,1}=\tau^{(p)}{}_0\exp(Q_l/kT)$ and $\tau^{(p)}_{l,2}=\tau^{(p)}{}_0\exp(Q_{l+1}/kT)$, where Q_l and Q_{l+1} are lower and upper limits of the lth box, respectively. $\Delta Ei^{(p)}{}_l(t)=Ei^{(p)}{}_{l+1}(t)-Ei^{(p)}{}_l(t)$, where $Ei^{(p)}{}_l(t)$ is an exponential integral for the lth box.[14]

The amplitude of the lth box in the distribution of AEs was calculated by the relation

$$P^{(p)}(Q_l)=\frac{\Delta r_l^{(p)}}{\sum_{l=1}^{n}\Delta r_l^{(p)}}. \quad (12)$$

$\Delta r_l^{(p)}$ describes the contribution of the pth MR process from the lth activation energy interval to the total relaxation. $P^{(p)}(Q_l)$ represents probability with which the pth relaxation process with activation energies from the lth interval contributes to the total pth type MR.

RESULTS

Investigation of the time-temperature dependent directional reordering that takes place in the MR of a structure can be made by the MAE technique. In particular, isochronal measurements are frequently used for separation of different MR processes dominant over different temperature ranges.[15] When performing analyses at the atomic scale level, we can find basic differences in the directional ordering behavior of the Fe-B, Fe-Si, Co-B, and/or Co-Si pairs in the amorphous $Fe_{75}Si_{15}B_{10}$ and $Co_{70}Fe_5Si_{15}B_{10}$ alloys. The elements constituting these pairs are frequently used in the amorphous soft magnetic alloys which are central to basic research and technological interests.

Generally, true continuous distribution functions of the activation energies $P^{(p)}(Q)$ for R relaxation processes in amorphous alloys are not mathematically expressible. They can, however, be approximated by a stepwise set of "n" box-type distribution functions with the constant $P^{(p)}(Q_l)$ in the lth energy interval (Q_l,Q_{l+1}). The distribution functions can be obtained by computer fitting of the MAE spectra (11).

Figure 4(a) presents the MAE spectrum for the as-cast amorphous $Fe_{75}Si_{15}B_{10}$ alloy. The isochrone with the time $t_2=180$ s after demagnetization shows a single MAE peak at the temperature $T=450$ K and the MAE intensity $\Delta r/r=57.7\%$. This is contrary to the double-peak MAE spectrum of the amorphous $Co_{75}Si_{15}B_{10}$ alloy.[14] The MAE peak is well below the Curie temperatures of this alloy, $T_C(Fe_{75}Si_{15}B_{10})=713$ K. The halfwidth of the MAE spectrum is relatively wide, $\Delta T=150$ K, which is typical for an MR with more than one elementary relaxation process. This fact is supported by the elongated form of the lowest isochrone with $t_2=2$ s.

According to the results of Ref. 16, it is reasonable to analyze relaxation in the Fe-based alloy containing both B

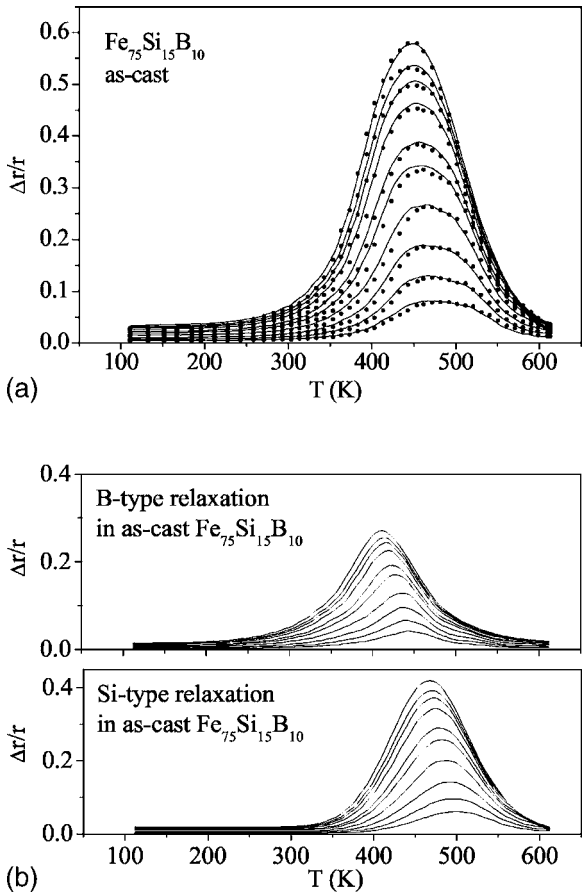

FIG. 4. (a) The total MAE spectrum of the as-cast FeSiB amorphous alloy with the measuring times $t_1=1$ s and $t_2=2$, 3, 5, 10, 20, 30, 60, 90, 120, and 180 s for curves from below up. (b) The MAE subspectra for the B- and Si-type magnetic relaxations, respectively, with measuring times t_1 and t_2 as in (a).

and Si elements with two distributions of AEs even though the spectrum has only one relaxation peak. By computer analysis with the help of Eq. (11), at the option $R=2$, the total MAE spectrum was split into two MAE subspectra characterizing two alloys,[12,17] we have identified that the subspectrum with a peak at 411 K originates from B-type MR. This B-type MR is caused by reorientation of the Fe-B atom pairs. The subspectrum with the peak localized to 467 K is related to the Si-type MR of the Fe-Si atom pairs [see Fig. 4(b)].

The AE spectra of the amorphous soft magnetic alloys characterize their MR kinetics. In the case of the amorphous FeSiB alloy, its AE spectrum consists of two AE subspectra for the B- and Si-type MRs, respectively (Fig. 5). The AE subspectrum for the B-type MR in the as-cast $Fe_{75}Si_{15}B_{10}$ alloy has the most probable activation energy $Q^*=1.33$ eV and the pre-exponential factor $\tau_0=2\times10^{-15}$ s. The Si-type MR in this FeSiB alloy, caused by the ordering of Fe-Si pairs, has activation parameters $Q^*=1.55$ eV and $\tau_0=6\times10^{-16}$ s. Parameters of the MAE and AE spectra of both of the investigated amorphous alloys in the as-cast and annealed states, respectively, are summarized in the Table I.

Low temperature annealing can introduce large changes to the atomic structure of amorphous alloys. The investigated

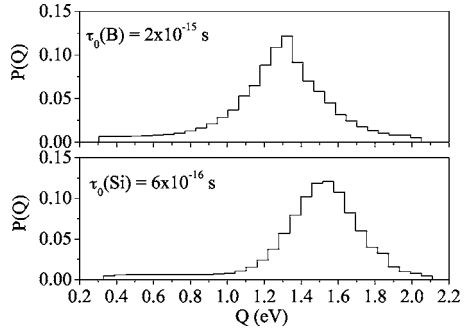

FIG. 5. Distributions of the activation energies $P(Q)$ and pre-exponential factors τ_0 of the B- and Si-type magnetic relaxation processes, respectively, in the as-cast amorphous FeSiB alloy, obtained by computer analysis of the relevant MAE subspectra [Fig. 4(b)].

$Fe_{75}Si_{15}B_{10}$ alloy was annealed at 723 K for 30 min. Its total MAE spectrum is presented in Fig. 6(a). In comparison to the as-cast state, the position of the single-peak MAE spectrum of the annealed alloy is shifted by 102 to 552 K and its MR intensity is lowered from 58 to 21%.

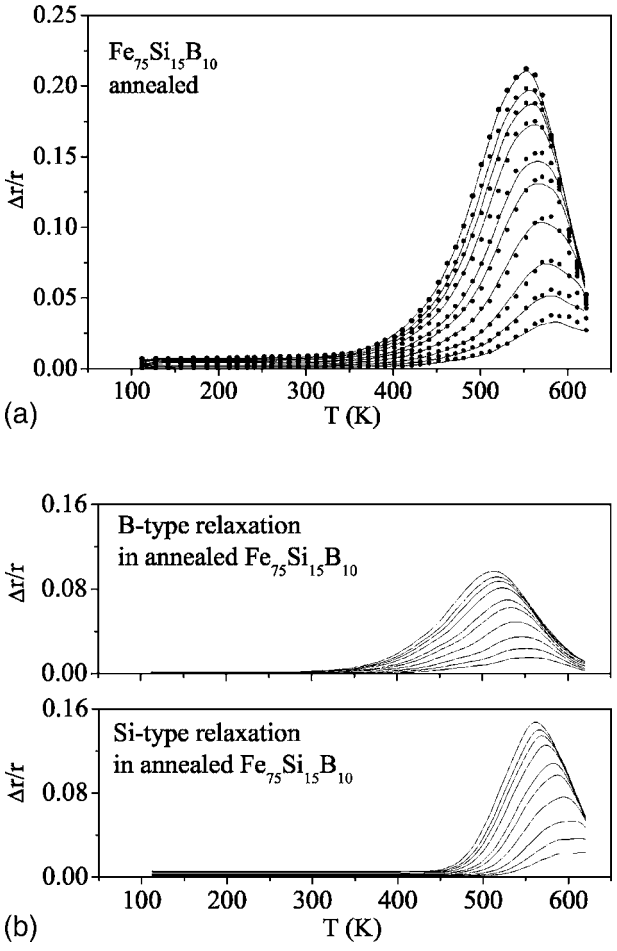

FIG. 6. (a) The total MAE spectrum of the annealed FeSiB amorphous alloy with measuring times t_1 and t_2 as in Fig. 4. (b) The MAE subspectra for the B- and Si-type magnetic relaxations, respectively.

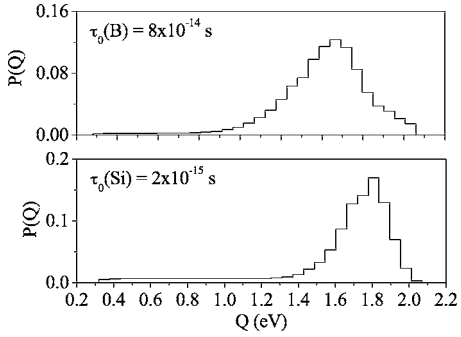

FIG. 7. Distributions of the activation energies $P(Q)$ and the pre-exponential factors τ_0 for the B- and Si-type magnetic relaxation processes, respectively, in the annealed amorphous FeSiB alloy, obtained from the relevant MAE subspectra [Fig. 6(b)].

The total MAE spectrum was split by computer analysis into two MAE subspectra characterizing the B- and Si-type particular MR processes [Fig. 6(b)]. After annealing, the peaks of the MAE subspectra for both B-type and Si-type MRs are also shifted by 102 and 95 K to the temperatures 513 and 562 K, respectively [Fig. 6(b) and Table I].

Shifts of the MAE subspectra of the annealed FeSiB alloy to higher temperatures seem to be contingent on shifts of the AEs to higher values. The computer analysis of the MAE spectrum [Fig. 6(a)] by the fitting function (11) gives two AE subspectra (Fig. 7) for the B- and Si-type MRs. The most probable activation energies Q^* for these MRs are increased by 0.13 and 0.26 eV to values of 1.46 and 1.81 eV, respectively, after annealing (Table I). In the case of the MRs in the $Co_{75}Si_{15}B_{10}$ alloy, the Q^*-s were increased by only 0.08 and 0.05 eV.[14] These values indicate that the Fe-based amorphous structure is more sensitive to annealing than the Co-based one. At the same time, the relevant pre-exponential factors τ_0 for the annealed FeSiB samples increased to 8×10^{-14} and 2×10^{-15} s for the B- and Si-type MRs, respectively. The AE subspectrum for the Si-type MR became asymmetrical.

The MR of the almost nonmagnetostrictive $Co_{70}Fe_5Si_{15}B_{10}$ amorphous alloy is of great interest to magneticians. The magnetic properties of this alloy are greatly improved by heat treatment. The investigated alloy contains fourteen times more Co than Fe and, naturally, its behavior is more characteristic of Co-based amorphous alloys than of Fe-based ones. Contrary to the FeSiB alloy, the total MAE spectrum [Fig. 8(a)] of the as-cast CoFeSiB alloy shows two peaks. The peaks of 17.7 and 5.6% heights are situated at 430 and 573 K, respectively. The MAE spectrum of the $Co_{70}Fe_5Si_{15}B_{10}$ alloy is similar to, but not identical with, that of the $Co_{75}Si_{15}B_{10}$ alloy.[14] It is shifted to higher temperatures compared to the MAE spectrum of the CoSiB alloy. As with the CoSiB alloy, the first MAE peak originates in the B-type MR and the second one in the Si-type MR.

The computer analysis of the total MAE spectrum by Eq. (11) gives two MAE subspectra [Fig. 8(b)] with relevant AE subspectra. The MAE subspectrum attributed to the B-type MR reaches its maximum value at 430 K and intensity 16.8%. The B-type MR in the as-cast CoFeSiB alloy is situated at a higher temperature than the observed B-type MRs

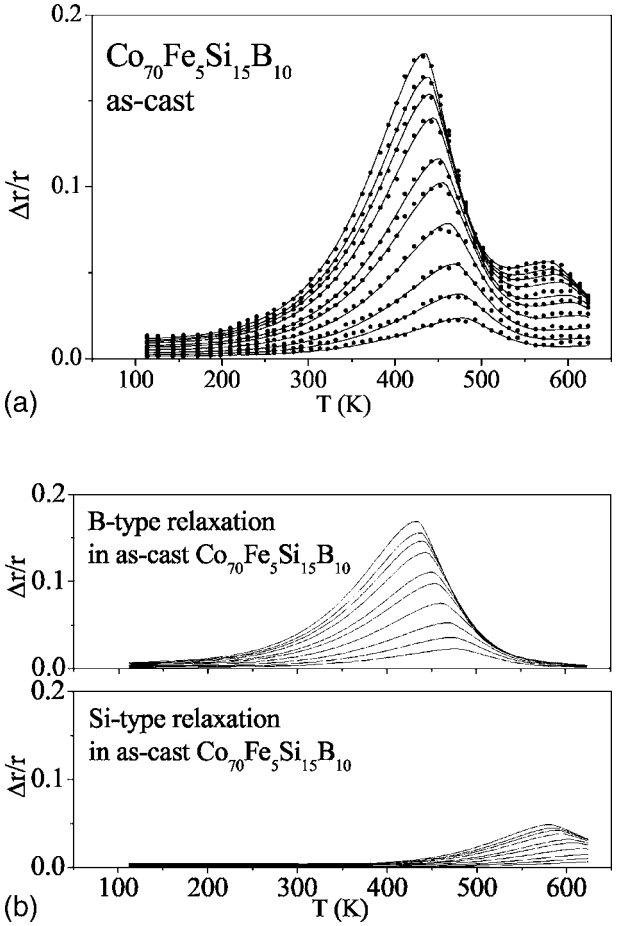

FIG. 8. (a) The total MAE spectrum of the as-cast CoFeSiB amorphous alloy with measuring times t_1 and t_2 as described in Fig. 4. (b) The MAE subspectra for the B- and Si-type magnetic relaxations, respectively.

in as-cast CoSiB and FeSiB alloys (Table I and Ref. 14). The MAE subspectrum attributed to the Si-type MR has a peak of 4.9% intensity situated at 575 K.

The AE subspectra obtained from the respective MAE subspectra are presented in Fig. 9. The B-type MR is characterized by the most probable activation energy $Q^* = 1.38$ eV and the pre-exponential factor $\tau_0 = 8 \times 10^{-16}$ s. The

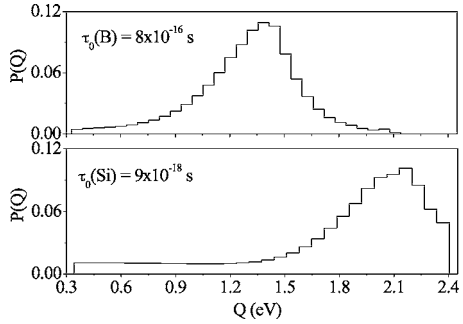

FIG. 9. Distributions of the activation energies $P(Q)$ and the pre-exponential factors τ_0 for the B- and Si-type magnetic relaxation processes, respectively, in the as-cast amorphous CoFeSiB alloy, obtained from the relevant MAE subspectra [Fig. 8(b)].

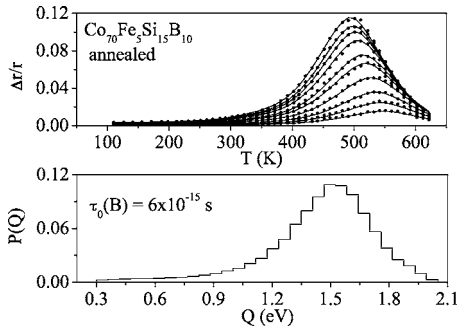

FIG. 10. (a) The MAE spectrum of the annealed $Co_{70}Fe_5Si_{15}B_{10}$ alloy with measuring times t_1 and t_2 as in Fig. 4. (b) The AE distribution $P(Q)$ and the pre-exponential factor τ_0 obtained from Fig. 10(a).

second MAE subspectrum obviously has an asymmetrical form. It belongs to the Si-type MR characterized by $Q^*=2.16$ eV and $\tau_0=9\times10^{-18}$ s. All activation parameters are of higher values than those for the CoSiB alloy.[14]

After annealing, the MAE spectrum of $Co_{70}Fe_5Si_{15}B_{10}$ is possessed only of a single peak in the investigated temperature range up to 620 K [Fig. 10(a)]. This behavior of the CoFeSiB alloy is different from that of the CoSiB alloy. The peak is situated around 500 K and has an intensity of 11.3%. We did not succeed in dividing the MAE spectrum into two MAE subspectra with B- and Si-type AE subspectra. Accordingly, the MAE spectrum [Fig. 10(a)] can be classified as a B-type MR. The most probable AE of the relevant AE spectrum is $Q^*=1.50$ eV and the pre-exponential factor $\tau_0=6\times10^{-15}$ s [see Fig. 10(b)].

DISCUSSION

A MAE spectrum is characterized by the MAE intensity, by the number of peaks, and by the locations of those peaks in the temperature scale. The investigated amorphous as-cast $Fe_{75}Si_{15}B_{10}$ and $Co_{70}Fe_5Si_{15}B_{10}$ alloys show completely different MAE spectra (Figs. 4 and 8). A comparison of values of activation parameters, temperatures of the MR maxima as well as MR intensities, reveals significant differences between both MR types in the Fe-based and Co-based alloys (Table I). These differences might reflect compositional and also possibly structural inequalities in the two investigated alloys.

The ternary amorphous $Fe_{75}Si_{15}B_{10}$ alloy shows a single-peak MAE spectrum, in contrast to the ternary $Co_{75}Si_{15}B_{10}$ alloy.[14] Two heterogeneous nearest-neighbor atom pairs with Fe, which take part in the MR, can be found in the FeSiB alloy. They are the Fe-B and Fe-Si pairs. The B-B, B-Si, and Si-Si pairs can be excluded because their interaction energies are not magnetic. It is also assumed that the only pairs containing a metalloid atom can contribute to MR within the investigated temperature range because M atoms are light and relatively mobile when compared with T atoms.

The MAE with a single peak at about 370 K, similar to the first MAE subspectrum of the $Fe_{75}Si_{15}B_{10}$ alloy, was found in the binary amorphous Fe-B alloys.[12,18] In these cases, the MRs can be attributed to reorientations of the Fe-B atom pairs. It was concluded in Ref. 19 that MR in crystalline Fe-Si at temperatures exceeding room temperature is connected with the reorientation of the Fe-Si pairs. In Ref. 20, the authors reported the MAE spectrum of crystalline Fe-Si alloy with a MAE peak at a temperature comparable to the temperature of the MAE peak in the MAE spectrum of our FeSiB alloy.

In view of the foregoing, a computer analysis of the MAE spectrum [Fig. 4(a)] was performed with two pre-exponential factors, one associated with reordering of pairs containing B (B-type MR) and second one associated with reordering of pairs with Si (Si-type MR). Two subspectra were obtained from the analysis of the measured MAE spectrum. Each subspectrum is connected with a particular MR process.

We have compared these subspectra with the subspectra of the amorphous CoSiB alloy. We have concluded that atom pairs can be arranged in the order Fe-B, Co-B, Fe-Si, and Co-Si by the increasing temperature of the MR maxima. A similar order is obtained when arranging the atom pairs by the increase of the most probable AE required for directional reordering. Fe-B pairs require the lowest AE for reordering. Most stable are pairs of Co-Si. There are other reasons that might explain the observed behavior. First, B atoms are lighter than Si atoms and can be moved more easily. Hence the T-B pairs have lower AEs than T-Si pairs. The variance in B-type MR in Co-based and Fe-based alloys can also be attributed to the different nature of Co-B and Fe-B chemical bonds.[21] Chemical affinity between elements constituting the pair contributes to the heights of the potential barrier, which must be overcome when a metalloid atom changes its position to an energetically more favorable one.

When an atom changes its position, chemical bonds to surrounding atoms at position $j=1$ are broken and the new ones are formed at position $j=2$. The stronger the bonds, the higher the temperature (activation energy) required to break them. A similar situation applies in the case of the Si-type MR: strong chemical affinity was found between Co and Si by extended x-ray-absorption fine structure (EXAFS) spectroscopy;[22] this supports our results obtained by MAE spectroscopy.

Additional important parameters acting in directional reordering processes are magnetic interaction energies. They have a primary impact on the time-temperature behavior of atom pairs. According to Eq. (2), three types of magnetic interaction energies are of importance. Magnetoelastic energy is macroscopically related to the saturation magnetostriction constant λ_S. Amorphous Co-Si-B alloys have negative λ_S,[23,24] as opposed to positive λ_S of the Fe-B and Fe-Si-B alloys.[9,23] This indicates significant influence of alloy composition (atom pairs compositions) on magnetoelastic interactions between atom pairs and local magnetizations.

Induced magnetic anisotropy has the same atomic scale origin as the MAE. It is macroscopically characterized by the constant of induced anisotropy, K_U. Its compositional dependence was experimentally investigated in Refs. 25 and 26. Roughly three times higher value of K_U was found in Co-B alloys than in Fe-B alloys.[23] Therefore, the composition of constituent elements has a great impact on magnetic anisotropy energy. Magnetic exchange energy depends on exchange integrals between magnetic atoms, hence inequalities

can be found between Co-based and Fe-based atoms.

We have analyzed above the directional ordering of atom pairs in the T-M_1-M_2 (FeSiB) alloy. The analysis was simplified by the compositional short-range order, where only T atoms surrounded the metalloid atom. The presence of two T elements in the alloy complicates the analysis. An amorphous $Co_{70}Fe_5Si_{15}B_{10}$ alloy contains a multitude of local environments of metalloid atoms. Where c is the mean coordination number of metalloid, the nearest neighborhood of the M atom may have the composition $Co_{c-x}Fe_x$, $x=0,\ldots c$. In that case it is difficult to distinguish between reorientations of Co-M and Fe-M pairs, hence analysis will be done on the level of clusters. Now B-type MR describes the directional ordering of both Co-B and Fe-B pairs; similarly, Si-type MR will reflect reordering of Co-Si and Fe-Si pairs. According to the concentration of Co and Fe elements in an investigated alloy, all clusters will contain Co.

Differences between the MAE spectra of $Co_{70}Fe_5Si_{15}B_{10}$ and $Co_{75}Si_{15}B_{10}$ (Ref. 14) may be attributed to the presence of Fe-B and Fe-Si atom-pairs, which were introduced to the $Co_{75}Si_{15}B_{10}$ alloy by the addition of Fe. The MAE spectrum peaks of the CoFeSiB alloy are shifted to higher temperatures when compared to the peak temperatures of the CoSiB MAE spectrum.

Magnetoelastic interaction energy seems to have greatest influence on the intensity of MAE processes. There are substantial differences between MR intensities $(\Delta r/r)_{\max}$ of $Fe_{75}Si_{15}B_{10}$ and $Co_{70}Fe_5Si_{15}B_{10}$ alloys [Figs. 4(a) and 8(a)]. Also, reluctivity changes caused by particular MR processes are different (Table I). According to Eq. (9), reluctivity change is proportional to magnetic term $\langle(\varepsilon_{eff}^{(p)})^2\rangle/I_S^2$ and to concentration of mobile defects $N_0^{(p)}\langle 1/\cosh^2(\Delta_S/kT)\rangle$. These two terms are independent, so the analysis of the impact of directional ordering on the reluctivity change is complicated. One can assume a higher concentration of T-Si pairs than T-B ones due to the higher amount of Si in the alloys. Both investigated alloys were prepared under the same technological conditions. If one assumes that the concentration of mobile Co-B pairs in $Co_{70}Fe_5Si_{15}B_{10}$ alloy is comparable to the concentration of mobile Fe-B pairs in $Fe_{75}Si_{15}B_{10}$, and a similar assumption is made for the concentration of Co-Si and Fe-Si pairs, then differences in MR intensities of the B(Si)-type MRs in $Co_{70}Fe_5Si_{15}B_{10}$ and $Fe_{75}Si_{15}B_{10}$ alloys are directly proportional to differences in magnetic terms. The main difference can be explained by the different magnetic interaction energies because the comparable values of I_S can be assumed for both the samples in the temperature range where the MRs take place. From three different interaction energies, which contribute to $\langle(\varepsilon_{eff}^{(p)})^2\rangle$ (2a), possibly magnetoelastic energy is of the greatest importance, because there are significant differences in the absolute values of λ_S for Co-based alloys ($|\lambda_S|<10^{-6}$) and for Fe-based alloys ($|\lambda_S|>30\times10^{-6}$).[10,23] Thus our result is consistent with the predictions of the MAE magnetoelastic model.[10]

According to the relationship $\langle(\varepsilon^{el(p)})^2\rangle\approx\lambda_S{}^2$,[7,9] magnetoelastic interactions are weakest in the $Co_{70}Fe_5Si_{15}B_{10}$ alloy, which has a λ_S value close to zero. Higher temperature is required to enable reorientations of atom pair axes due to low total magnetic interaction energy. This is probably the reason why both B-type and Si-type atom-pairs are more stable in the $Co_{70}Fe_5Si_{15}B_{10}$ alloy when compared with other investigated alloy (see values of $T_{MAX,AC}$ and Q_{AC}^* in Table I).

The value of the pre-exponential factor τ_0 is sensitive to atomic configurations around a relaxing atom pair, which is expressed by the entropy term $S^{(p)}$ (4). τ_0 in crystalline alloys is about 10^{-13} s,[15] which is the reciprocal value of the Debye frequency. The τ_0 for the reversible MR processes in amorphous alloys are lower than 10^{-13} s. Several conclusions may be drawn from the obtained τ_0 values. Co-M pairs have lower τ_0 values than Fe-M pairs. This might be explained by the different nature of the nearest neighborhood of a metalloid atom when Co atoms or Fe atoms surround it. T-B pairs have greater τ_0 values than T-Si pairs. This is probably due to the diverse diameters of B and Si atoms and different mean inter-atomic distance.[27]

Since annealing does not dramatically change the magnetic term in Eq. (9), the reduction of the maximum MR intensities are connected to the reduction of the concentration of mobile atom pairs. During annealing in the paramagnetic state, the amorphous structure undergoes large changes. In this case, short-range ordering is driven by the structural term Δ_S. Free volumes are partly annealed out and chemical affinities between elements can cause changes in compositional short-range order. These changes are macroscopically reflected in the MAE spectra of the annealed samples. The impact of annealing on the free volume release is probably the main reason for observed changes in values of the most probable AEs and temperatures of the MR maxima: the smaller the free volumes, the larger the AEs.

A greater lowering of maximum MR intensities after annealing was observed for MRs in the $Fe_{75}Si_{15}B_{10}$ alloy than in the $Co_{70}Fe_5Si_{15}B_{10}$ alloy (Table I). It can be assumed that a greater amount of free volume was annealed out from the FeSiB alloy than from the CoFeSiB alloy. The smaller amount of free volumes results in smaller concentrations of movable atom pairs $N_0^{(p)}$, which in turn results in a smaller MAE intensity $(\Delta r/r)_{\max}$.

Two situations may appear with respect to B-type and Si-type MRs in the annealed $Co_{70}Fe_5Si_{15}B_{10}$ alloy. A single-peak MAE spectrum may be due to the superposition of two MAE peaks or the Si-type MAE peak is shifted to higher temperatures and does not contribute to the experimentally observed one. Our attempt to split the MAE spectrum into two subspectra by computer analysis was not successful. We conclude that the observed MAE peak is a result of B-type MR and that the contribution of Si-type MR at the investigated temperature range is negligible. The pre-exponential factor for the B-type MR in the annealed $Co_{70}Fe_5Si_{15}B_{10}$ alloy has a value of 6×10^{-15} s, which falls between values observed for B-type MRs in annealed $Co_{75}Si_{15}B_{10}$ and $Fe_{75}Si_{15}B_{10}$ alloys.

After annealing, all pre-exponential factors τ_0 in the $Fe_{75}Si_{15}B_{10}$ and $Co_{70}Fe_5Si_{15}B_{10}$ alloys increase (Table I) and approach to 10^{-13} s. This can be explained by a decrease in entropy (5) caused by an increase of the structural short-range order, which after annealing is closer to the structural order typical for crystalline alloys.[15]

CONCLUSION

Theoretical and experimental elements of a nonconventional computer-supported spectroscopic method—the magnetic aftereffect spectroscopy—providing sets of basic activation energy spectra of the magnetic relaxation processes, were presented. The magnetic aftereffect investigations were performed in a temperature range of 77–620 K on two representative amorphous alloys $Fe_{75}Si_{15}B_{10}$ and $Co_{70}Fe_5Si_{15}B_{10}$ in the as-cast and annealed states. The extended micromagnetic model was used for computer analysis of the observed MAE spectra.

The B- and Si-type magnetic relaxations with different activation parameters were proven in the FeSiB and CoFeSiB alloys. In the as-cast FeSiB alloy, the two most probable activation energies, $Q^*=1.33$ and 1.55 eV, with the pre-exponential factors $\tau_0=2\times10^{-15}$ and 6×10^{-16} s, were obtained for the B- and Si-type MRs, respectively. They are caused by reorientations of the Fe-B and Fe-Si atom pair directions. In the as-cast CoFeSiB alloy, the B- and Si-type MRs are predominantly caused by the Co-B and Co-Si atom pair reorientations. They are characterized by the activation energies $Q^*=1.38$ and 2.16 eV and the pre-exponential factors $\tau_0=8\times10^{-16}$ and 9×10^{-18} s, respectively. The directional ordering behavior of different atom pairs and differences in activation parameters are attributed to several aspects: magnetic interaction energies, chemical affinities between atom pairs and surrounding atoms, mean interatomic distances, and weights and sizes of the relaxing elements. Atom pairs Fe-B, Co-B, Fe-Si, and Co-Si were aligned by the increasing values of the most probable activation energies of the MRs.

The high-magnetostrictive amorphous FeSiB alloy shows much higher MAE intensity than that of the almost nonmagnetostrictive CoFeSiB alloy.

Low temperature annealing causes lowering of the MAE peaks and shifts the peak temperatures and the activation energies of MRs in both alloys to higher values. These results support the free volume conceptions of the MR in the amorphous alloys.

The amorphous $Fe_{75}Si_{15}B_{10}$ alloy is more sensitive to annealing than $Co_{70}Fe_5Si_{15}B_{10}$. The annealed CoFeSiB alloy has a single relaxation peak only, which predominantly originates from the B-type magnetic relaxation.

ACKNOWLEDGMENTS

This work was partly supported by VEGA agency under Grant No. 1/1017/04. R. O'Handley is acknowledged for his continuing interest in our work. R. Varga is acknowledged for valuable discussions.

*Corresponding author. Electronic address: pavol.vojtanik@upjs.sk
†Present address: BSH Drives and Pumps s.r.o., Vysokoskolska 8, 04001 Kosice, Slovakia.

[1] K. I. Arai and N. Tsuya, IEEE Trans. Magn. **MAG-13**, 1550 (1977).
[2] H. Kronmüller, N. Moser, and F. Rettenmeier, IEEE Trans. Magn. **20**, 1388 (1984).
[3] J. Degro, P. Vojtanik, J. Filipensky, and P. Duhaj, J. Magn. Magn. Mater. **117**, 251 (1992).
[4] D. B. Miracle, Nat. Mater. **3**, 697 (2004).
[5] R. Hasegawa, J. Optoelectron. Adv. Mater. **4**, 173 (2004).
[6] H. Kronmüller and M. Fähnle, *Micromagnetism and the Microstructure of Ferromagnetic Solids* (Cambridge University Press, Cambridge, 2003), p. 274.
[7] H. Kronmüller, Phys. Status Solidi B **127**, 531 (1985).
[8] R. Andrejco and P. Vojtanik, J. Phys.: Condens. Matter **16**, 3745 (2004).
[9] P. Allia and F. Vinai, Phys. Rev. B **26**, 6141 (1982).
[10] P. Allia and F. Vinai, Phys. Rev. B **33**, 422 (1986).
[11] P. Vojtanik, D. Macko, and A. Lovas, IEEE Trans. Magn. **30**, 476 (1994).
[12] F. Rettenmeier, E. Kisdi-Koszo, and H. Kronmüller, Phys. Status Solidi A **93**, 597 (1986).
[13] F. Walz, Phys. Status Solidi A **82**, 179 (1984).
[14] P. Vojtanik, R. Andrejco, and R. Varga, Phys. Rev. B **70**, 052407 (2004).
[15] H. Blythe, H. Kronmüller, A. Seeger, and F. Walz, Phys. Status Solidi A **181**, 233 (2000).
[16] A. Böhönyey, G. Huhn, L. F. Kiss, A. Lovas, and I. Geröcs, J. Non-Cryst. Solids **232-234**, 490 (1998).
[17] T. Miyazaki, M. Takahashi, and K. Hisatake, J. Appl. Phys. **57**, 3575 (1985).
[18] P. Vojtanik and I. B. Kekalo, Phys. Status Solidi A **60**, K45 (1980).
[19] R. S. Turtelli, E. de Morais, G. Wiesinger, Ch. Reichl, Vo Hong Duong, and R. Grössinger, J. Magn. Magn. Mater. **205**, 290 (1999).
[20] J. Zbroszczyk, W. H. Ciurzynska, Y. Tanaka, M. Enokizono, J. Olszewski, and M. Hasiak, J. Magn. Magn. Mater. **160**, 141 (1996).
[21] B. W. Corb, R. C. O'Handley, and N. J. Grant, Phys. Rev. B **27**, 636 (1983).
[22] M. L. Fdez-Gubieda, I. Orue, F. Plazaola, and J. M. Barandiarán, Phys. Rev. B **53**, 620 (1996).
[23] T. Miyazaki and M. Takahashi, J. Magn. Magn. Mater. **42**, 29 (1984).
[24] M. Vázquez, E. Ascasibar, A. Hernando, and O. V. Nielsen, J. Magn. Magn. Mater. **66**, 37 (1987).
[25] J. Gonzalez, J. M. Blanco, I. Telleria, J. M. Barandiarán, M. Vázquez, A. Hernando, and A. R. Pierna, J. Magn. Magn. Mater. **83**, 168 (1990).
[26] F. E. Luborsky, in *Ferromagnetic Materials* edited by E. P. Wohlfarth (North-Holland, London, 1980), Vol. 1, p. 507.
[27] Y. Takahara and N. Narita, Mater. Sci. Eng., A **315**, 153 (2001).